Maximizing Aggregate Throughput in 802.11 Mesh Networks with Physical Carrier Sensing and Two-Radio Multi-Channel Clustering

Jing Zhu[1], Sumit Roy[1], Xingang Guo[2], and W. Steven Conner[2]
{zhuj, roy}@ee.washington.edu
{xingang.guo, w.steven.conner}@intel.com
[1] Department of Electrial Engineering, University of Washington, Seattle, WA, U.S.A.
[2] Communications Technology Lab, Intel Corporation, Hillsboro, OR, U.S.A.

***Abstract*— Spatial reuse in a mesh network allows multiple communications to proceed simultaneously, hence proportionally improving the overall network throughput. To maximize spatial reuse, the MAC protocol must enable simultaneous co-channel transmitters to maintain a separation distance that is sufficient to avoid interference. Within that distance, a set of orthogonal channels is employed by different links. This paper demonstrates that physical carrier sensing enhanced with a tunable sensing threshold is effective at avoiding co-channel interference in 802.11 mesh (static + multi-hop) networks. Moreover, for multi-channel mesh networks, an architecture for channel clustering based on two-radio nodes is proposed. Distributed clustering is achieved using the Highest-Connectivity Cluster (HCC) algorithm. All inter-cluster communications are performed on a common channel using the default radio, while intra-cluster communications use the secondary radio with channel selection based on a new Minimum Interference Channel Selection (MIX) algorithm that minimizes the co-channel interference (CCI). Backward compatibility is guaranteed by allowing legacy single-channel devices to connect to the new two-radio devices through the common default radio. Simulation results for large-scale 802.11b and 802.11a networks demonstrate the significant improvement in one-hop aggregate throughput. Specifically, the new two-radio multi-channel mesh solution increases the aggregate throughput by more than twice w.r.t. the traditional single-radio single-channel mesh.**

I. Introduction

The past few years have witnessed the rapid proliferation of wireless LANs in various environments: home, enterprize and hotspot. The need for higher data rates and improved coverage has led to multi-cell networks (particularly for business and hotspot scenarios but also for clusters of homes/apartments) where each cell is served by its own access point (AP). Currently, all APs are directly connected (typically via Ethernet) to an Internet gateway. Therefore, the cost and time of deploying a large scale WLAN network dramatically increases as the network expands. A possible solution to this problem is connecting APs wirelessly to form a (static) multi-hop .11 (*mesh*) network (see Fig.1). The high interest in such an approach is indicated not only by the newly formed Mesh Task Group within IEEE 802.11 but also mesh solutions offered by several companies [2], [3], [4] to list a few. Such a future *wireless AP-AP mesh network* requires both protocol and architectural extensions to current .11 networks for which there does not exist any standardized inter-AP connectivity protocol. Furthermore, since the wireless channel is a broadcast (shared) medium with bandwidth limitations, the aggregate throughput of such a wireless inter-AP mesh is governed by the following key network parameters:

- K: number of concurrent active links per channel (degree of co-channel spatial reuse);
- W: max. data rate per channel;
- N: number of orthogonal channels within a reuse distance

This paper looks at approaches to maximize K as well as utilizing N to maximize the aggregate throughput of a wireless mesh network.

In [7], spatial reuse was demonstrated to depend on various characteristics of the network, including the type of radio, network topology, channel quality requirements and signal propagation environment. For a given network configuration, there exists a minimum separation distance such that when simultaneous transmitters are separated by that distance, the maximum number of simultaneous transmissions can be accommodated, allowing maximum network throughput to be achieved. However, achieving maximum spatial reuse would require an ideal MAC protocol that schedules communication to maintain the optimal transmitter separation distance (to minimize interference) in a fully distributed manner.

Nodes in a IEEE 802.11 WLAN network seeking channel access use carrier sensing to determine if the medium is available before transmitting to avoid packet collision [1]. Two types of carrier sensing are supported by the 802.11 MAC: mandatory physical carrier sensing that monitors the RF energy level in the air and optional virtual carrier sensing that uses the Request-to-Send/Clear-to-Send (RTS/CTS) handshake to ensure that the air medium at the receiver is reserved prior to data packet transmission. Virtual carrier sensing was designed to avoid the well-known hidden terminal problem [11], where it is assumed that physical carrier

sensing at a transmitter is not sufficient to avoid interference at a receiver. However, it has been shown that virtual carrier sensing via RTS/CTS in fact suffers from fundamental limitations in avoiding interference from hidden terminals [12]. In 802.11, this can be attributed to lack of proper design of the physical carrier sensing mechanism. In this paper we demonstrate that, when properly tuned, physical carrier sensing is effective at avoiding interference in a multi-hop wireless mesh network *without the use of virtual carrier sensing*.

Physical carrier sensing allows a station to assess the channel condition before transmitting to make sure that no interference can occur. A node samples the energy on the channel and initiates channel access only if the reading is below the carrier sensing threshold, indicating that any ongoing communication only produces tolerable interfere with the impending transmission. According to RF pathloss models, the long-term average received energy at a node decays with distance from a transmitter. Hence the carrier sensing threshold effectively determines the minimum allowed distance between simultaneous transmitters. Since the optimal distance depends on various network properties, the carrier sensing threshold should be tuned to current network conditions. However, many of today's 802.11 MAC implementations use a static threshold, or do not allow the threshold to be independently tunable [16]. As a result, physical carrier sensing often leads transmitters to be either too conservative or too aggressive when using the wireless channel.

In this work, we assume a tunable carrier sensing threshold and illustrate how to derive the appropriate carrier sensing threshold from relevant network characteristics via analysis. Furthermore, we propose an estimation-based adaptive physical carrier sensing scheme to automatically tune the threshold to a near-optimal value. We present OPNET simulation results for two regular network topologies (chain and grid) to validate the theoretical optimal PCS threshold. Our results further show that by tuning the physical carrier sensing threshold, without requiring virtual carrier sensing, the overall network throughput can be improved significantly compared to that of the legacy 802.11 MAC. The increased throughput can approach approximately 90% of the theoretical upper-bound predicted by spatial reuse models in a large chain. Simulation results also demonstrate the effectiveness of the estimation-based adaptive physical carriers sensing scheme in networks with dynamic topology and heterogeneous links.

We note that performance improvement of 802.11 networks based on enhancement to various aspects of the 802.11 MAC protocol has been the subject of recent work [10] [14]. For any given environment, optimizing network performance must be a careful combination of approaches addressing multiple aspects of network performance (e.g. throughput, fairness, etc.) which is beyond the scope of this work. We focus here specifically on *leveraging the spatial reuse* of mesh networks to enhance the throughput through physical carrier sensing, which is an essential requirement for achieving optimal aggregate throughput in a dense wireless network.

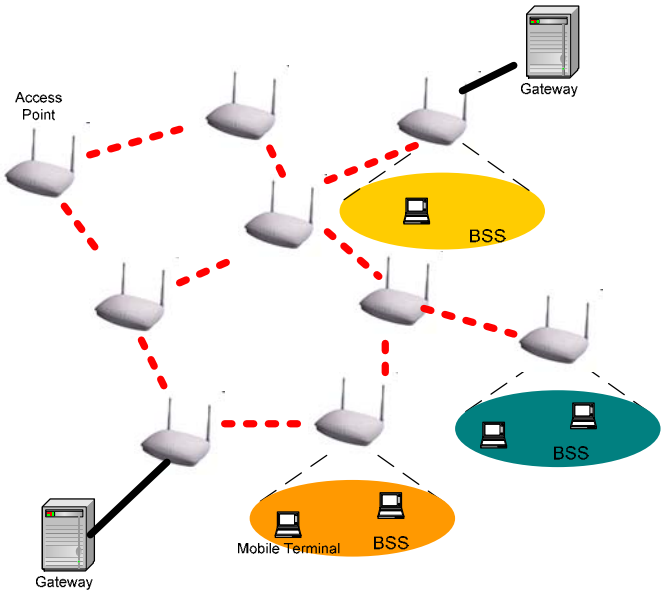

Fig. 1. Wireless AP-to-AP mesh Networks

Communication between nodes on the AP-mesh can share a single channel or use multiple narrower-band channels. This can be implemented readily using a single-radio network (all nodes have only one radio interface) that suggests the need for a single *wideband* shared channel for the entire AP-mesh to support many simultaneous transmissions. However, this approach has not been adopted by industry standards as yet and lacks hardware implementations [1]. Using multiple narrower-band channels entails potentially complicated channel assignment schemes to inter-AP links, but has existing hardware support (N=8 in 802.11 a, and N=3 in 802.11 b). Thus our proposed solution is based on using a $20MHz$ channel for all inter-AP communications while noting that this is likely to be a throughput bottleneck in situations where the inter-AP (routed) traffic dominates.

Two-radio multi-channel approaches, where each node is equipped with two similar PHY/MAC radio interfaces for AP-AP communication, can effectively exploit the available multiple orthogonal channels [2] which is infeasible with a one-radio AP Mesh with multiple narrowband channels. In a two-radio implementation, each node in the AP-mesh is equipped with two WLAN cards that are used for intra-cell and inter-cell communications, respectively. This will always provide higher throughput than a single-channel approach, since intra-AP traffic is now separated from inter-AP traffic made possible by two-radio nodes. Such a multi-radio architecture has been proposed in [27] where the channel used for any AP-AP link from among the available set is selected by sending probes to estimate the link round

[1]Further, proportionally improved MAC efficiency is needed to translate increase link layer rates to higher MAC throughput.

[2]Note that each AP also needs a third radio for communications for the AP-MT link (MT: Mobile Terminal), which must be orthogonal to the AP-AP mesh band to avoid interference. This promotes the use of dual, e.g. .11 a/b, radio interface cards.

trip time (RTT) for the available channels and choosing the one with minimum RTT. Updating the channel allocation is performed periodically every few seconds. While the RTT is a useful indicator of channel load, it is a less-than-adequate metric for estimating interference due to simultaneous transmissions in a wireless scenario. Thus [27] protocol operates more as a load-balancing scheme which improves but does not optimize aggregate network throughput.

Continuous monitoring of channel quality on all channels is infeasible with a single radio; two radios per node considerably simplifies this because this task can be performed by one radio while the other is transmitting data on the currently assigned channel. Suggestions for using one radio purely as a dedicated control channel and the other for data on all other channels have appeared for two-radio architectures [26] [25]; but these lead to low channel utilization due to control channel becoming a bottleneck, and offers no backward compatibility. Thus in our implementation, both radios are used to support data transmission. Nonetheless, irrespective of the specifics of how the two radios are used, this architecture allows the possibility of a *fully distributed* MAC implementation that is desirable for network robustness. For example, to eliminate the control channel bottleneck, we propose a new *semi-distributed* AP-clustering approach. A distributed Highest-Connectivity Cluster (HCC) algorithm [22] is employed to divide the network into AP clusters that are distinguished by the channel used for intra-cluster communication. Inter-cluster communication is performed using the (*default* and intra-cluster via the *secondary*) radio, respectively.

A common channel is used for all inter-cluster communications, and different channels are selected for intra-cluster communications by using a new Minimum Interference Channel Selection (MIX) algorithm. Control or management traffic uses only the default radio; while the secondary radio is only for data transmissions. Note that backward compatibility is achieved since this architecture allows a legacy single-radio AP to connect to the new two-radio APs through the (common) default radio.

Unlike most of other cluster-based networks (e.g. Bluetooth, UWB) that usually employ a cluster head as a controller running a centralized MAC, the architecture here uses clustering to only assign a channel in a distributed manner for the MAC; the base 802.11 MAC mechanisms are unchanged. Similar to [27], our protocol uses a virtual MAC address in place of the multiple physical MAC addresses used by two radios so that the higher (routing) layer sees only a single wireless network interface. Routing between the nodes is based on ad-hoc routing approaches similar to that in the traditional single-channel, single-radio mesh.

II. Related Work on .11 MAC Enhancements

Interference mitigation has been a well-known challenge for MAC protocols in wireless mesh networks. Much of the existing research in this space has focussed on eliminating the *hidden terminal* [11] problem. A virtual carrier sensing mechanism, implemented through the RTS/CTS handshake, has been adopted by IEEE 802.11 in an attempt to eliminate the hidden terminal problem. However, this has an underlying assumption that all hidden terminals are within transmission range of receivers (allowing them to receive the RTS or CTS packet successfully). While such an assumption may be reasonable for single cell WLANs, it is generally not true for multi-cell WLANs and multi-hop mesh networks. Researchers [12] [13] [14] have by now recognized that virtual carrier sensing with RTS/CTS does not solve the hidden terminal problem effectively for such networks.

It was shown in both [12] and [14] that the interference range is a function of T-R separation distance. Depending on the T-R separation distance, the interference range can be smaller or larger than the transmission range. If the interference range is smaller than the transmission range, RTS/CTS can indeed prohibit all the hidden terminals from interfering with the existing transmission; but some of the nodes that are not capable of interfering are also prohibited from transmitting. Thus, in this configuration RTS/CTS is too aggressive, resulting in a significant exposed terminal problem that wastes potential throughput by requiring potential transmitters to unnecessarily back off. On the other hand, if the interference range is larger than the transmission range, RTS/CTS can fail to prevent hidden terminals from interfering with an existing transmission. So RTS/CTS is too conservative and ineffective in this case.

A technique was suggested in [12] to avoid the conservative RTS/CTS scenarios by allowing only the transmitter-receiver pairs with distance shorter than a threshold to perform transmission; the threshold is set such that the corresponding interference range will not be larger than the transmission range. The constraint on T-R separation distance is imposed by only allowing a node to reply to a RTS packet with a CTS packet when the receive power of the RTS packet is larger than a threshold, even if the RTS packet is received successfully and the node is idle. This added constraint ensures that RTS/CTS never becomes too conservative and so the hidden terminal problem is avoided. However, this approach does not address the exposed terminal problem introduced by the aggressive RTS/CTS. Another disadvantage of such an approach is that it reduces effective transmission range and thus lowers network connectivity.

Several other techniques attempt to reduce inefficiencies introduced by exposed terminals. The protocol described in [10] focuses on the exposed terminal problem directly by enabling nodes to identify themselves as exposed nodes and opportunistically scheduling concurrent transmissions whenever possible. While [14] recognizes that RTS/CTS can be either too conservative or too aggressive, it only addresses the problems associated with aggressive RTS/CTS. The authors propose a Distance-Aware Carrier Sensing (DACS) scheme which employs an extra handshake in addition to RTS/CTS to disseminate one-hop distance information to neighbors so that medium reservation can be more accurate and spatial reuse can be improved to reduce

the negative impact of exposed terminals.

Besides interference, packet collision is another important factor contributing to the final SINR. However, collisions due to simultaneous transmission attempts cannot be reliably prevented by using physical carrier sensing alone. A common approach to avoiding persistent collisions is random back-off, e.g the binary exponential backoff algorithm in the 802.11 MAC standard. Recently, there have been several efforts aimed at optimizing the back-off algorithms and contention window size to minimize collisions [6] [17] etc. While the focus of this paper is on leveraging the spatial reuse of a network to enhance the throughput performance through physical carrier sensing, these techniques may be supplemented with the above to simultaneously minimize interference and the impact of packet collisions to further improve aggregate throughput in a dense wireless network.

Unlike prior techniques that attempt to avoid interference through handshake protocols, this paper approaches interference mitigation from the perspective of leveraging spatial reuse. We believe that the key to the optimal spatial reuse is to maintain the appropriate separation distance between simultaneous transmitters. Therefore we focus on enhancing the physical carrier sensing mechanism with tunable sensing threshold for the 802.11 MAC. What we propose in this paper is a simple and effective method that directly redresses some of the issues in virtual carrier sensing with RTS/CTS.

The rest of this paper is organized as follows: Section II presents a basic communication model for interference analysis and exposes the limitations of carrier sensing as currently implemented in 802.11 DCF. Section III introduces our suggestions for enhanced physical carrier sensing based on a tunable physical sensing threshold, and demonstrates the resulting throughput improvements for some regular mesh networks topologies. Section IV describes our novel two-radio multi-channel clustering architecture. Section V presents OPNET simulation results showing significant performance enhancements obtained from tuned physical carrier sensing along with new clustered two-radio, multi-channel AP-mesh. Section VI discusses our results in the context of related work, and Section VII concludes the paper.

III. Managing Interference with Physical Carrier Sensing (PCS)

In CSMA/CA based wireless networks such as IEEE 802.11 networks, a transmitter relies on carrier sensing to determine if the medium is 'available', i.e., has acceptable level of interference from ongoing transmissions. A transmission is initiated only if the energy level is below the PCS threshold. This section uses common radio propagation models to determine the effectiveness of carrier sensing and points out several shortcomings of the carrier sensing technique employed in 802.11 MAC protocol.

A. Communication Model

Path loss models are commonly used to describe the average received power at a receiver over a wireless medium [7] [19] as a function of the T-R (transmitter-receiver) radial separation, d, i.e.,

$$P_{rx}(d) = \bar{P}_{rx}(\frac{\bar{d}}{d})^{\gamma} \tag{1}$$

where γ is the path loss exponent that characterizes the rate of signal degradation with distance in the particular network environment. $P_{rx}(d)$ denotes the signal power at distance d from the transmitter and $\bar{P}_{rx}$ is the signal power measured at a reference distance $\bar{d}$ (usually 1 meter).

The aggregate energy at any receive node consists of desired signal, interference (from unwanted transmitter(s)) and background noise. A 802.11 node can receive a packet with high probability of success in additive noise only if the received signal strength is greater than a threshold (denoted by P_R, i.e. reception sensitivity); and equivalent condition in the presence of interference is that the received Signal-Interference and Noise-Ratio (SINR) exceeds a threshold denoted by S_0; i.e.,

$$\begin{cases} P_{rx}(d) \geq P_R \\ \frac{P_{rx}(d)}{P_N + \sum_i P_{rx}(d_i)} \geq S_0 \end{cases}, \tag{2}$$

where P_N is the background noise power, and $P_{rx}(d_i)$ denotes the power of interference source i at distance d_i from the receiver. 802.11 networks support multiple data rates, and a higher data rate requires a higher S_0.

B. Terminologies

Eq.2 provides constraints on the receive power as well as the SINR at detector input for successful detection. In the absence of any interference, the receive sensitivity P_R is set to satisfy $P_R/P_N > S_0$; this determines the *transmission range* or the maximum distance for successful reception in additive noise only. It is clear that the actual SINR perceived via PCS at a receive node will vary due to the presence of interference from ongoing transmissions.

Fig.2 shows a typical mesh network with a reference transmission from a node TX to a node RX in the presence of four other nodes (A, B, C, and E). The same transmission power is used by every node in the network. We define the following:

D: TX-RX separation distance, defines $P_D = P_{rx}(D)$.

R: Transmission range, given by

$$R = \bar{d}(\frac{\bar{P}_{rx}}{\max(P_R, S_0 P_N)})^{\frac{1}{\gamma}} = \bar{d}(\frac{\bar{P}_{rx}}{P_R})^{\frac{1}{\gamma}}, \tag{3}$$

I: Interference range – implies a single transmitter within that range of the receiver will disrupt reception of the desired transmitter, given by

$$I = D(\frac{1}{\frac{1}{S_0} - (\frac{D}{d})^{\gamma}\frac{P_N}{\bar{P}_{rx}}})^{1/\gamma}. \tag{4}$$

With negligible background noise, Eq.4 turns to

$$I \approx S_0^{1/\gamma} D. \tag{5}$$

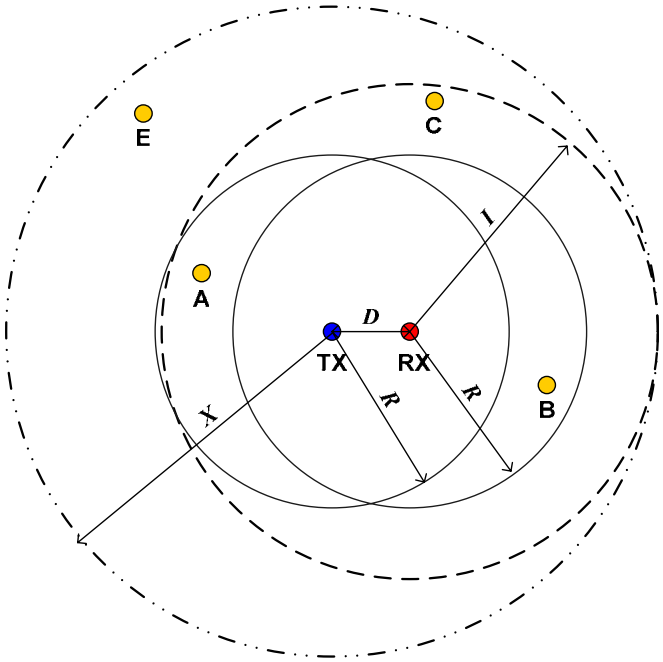

Fig. 2. Illustration of relative transmission and interference distances in a wireless mesh network.

X: Physical carrier sensing range – a node will be able to detect an existing transmitter within that range via physical carrier sensing, given by

$$X = \bar{d}(\frac{\bar{P}_{rx}}{P_C})^{\frac{1}{\gamma}}, \quad (6)$$

where P_C denotes the physical carrier sensing (PCS) threshold.

Table I briefly summarizes the common symbols used throughout this paper to describe carrier sensing.

C. Limitations of Carrier Sensing in 802.11 MAC Protocols

In today's 802.11 networks, the PCS scheme is typically configured with a fixed threshold, which is often set very low such that even a remote communication would force a station to withhold its transmission. Clearly, dynamic tuning of the PCS threshold according to current network conditions allows for optimum exploitation of spatial capacity.

In addition to PCS, 802.11 MAC also allows for virtual carrier sensing (VCS) scheme [1] for interference avoidance. This is accomplished by a initial Request-to-Send (RTS)/ Clear-to-Send (CTS) handshake prior to data transmission. With VCS, each station maintains a NAV (Network Allocation Vector) that indicates the period(s) during which the shared medium is reserved by other stations, hence it knows when NOT to transmit. When contending for the medium, a station broadcasts its intended transmission period in the RTS or CTS; each station that receives the broadcast updates its NAV. Hence, VCS requires participating stations to be able to receive and decode the RTS/CTS broadcast frames from any other stations in the network with which they may potentially interfere. Unfortunately, this requirement cannot be guaranteed in many scenarios

P_R	Received Power Threshold
P_C	Physical Carrier Sensing Threshold
P_D	Received Power at distance D
P_N	Background Noise Power
P_I	Interference Power
S_0	SNIR Threshold
γ	Path Loss Exponent
X	Physical Carrier Sensing Range
R	Transmission Range
I	Interference Range
D	Transmission Distance
p_{cs_t}	P_C/P_D (normalized CS threshold)
k	Spatial reuse factor
W	Link capacity

TABLE I

COMMON SYMBOLS FOR DESCRIBING PHYSICAL CARRIER SENSING.

[12] as exemplified in Fig. 2. The VCS scheme appropriately prevents nodes A and B from initiating an interfering transmission, as they are in the transmission range of TX and RX. But node C is too far away from both TX and RX to reliably receive and decode the RTS or CTS packets, yet it is still a potential hidden node that could interfere with the packet reception at RX.

IV. ENHANCING PHYSICAL CARRIER SENSING

A. Tuning Physical Carrier Sensing (PCS) to Avoid Interference

Physical carrier sensing allows a station to assess the channel conditions before transmitting to avoid interference that will lead to packet collisions. A station samples the energy level at the air interface and starts a packet transmission only if the energy level is below a threshold P_C, called the PCS threshold.

In a multi-hop wireless network, only a subset (of the overall nodes) belonging to a cluster share a common transmission medium on a contention basis. The fundamental factor that determines whether a packet can be successfully received is the SINR at the receiver. If the signal that a device is attempting to receive is sufficiently stronger than the background noise and interference, successful packet reception can occur even in the presence of interference. Thus, the goal of PCS is to prevent those simultaneous transmissions that will lead to packet collisions, while permitting other simultaneous transmissions that do not violate receive SNIR requirements and thus maximize spatial reuse.

Fig. 3 illustrates a simple example of how the choice of PCS threshold can impact wireless network performance. If the threshold is too high, the CSMA is needlessly conservative. While node C is transmitting, both nodes A and B will backoff as in Fig. 3(a) , even though node A may be able to simultaneously transmit without causing much interference at C's receiver to disrupt successful communication. On the other hand, as shown in Fig. 3 (b), if the threshold is too high so as to allow both nodes A and B to transmit simultaneously with C, excessive interference will be generated resulting in packet collisions. If the PCS threshold is appropriately configured, as shown in Fig. 3 (c), nodes A and C will be permitted to successfully transmit

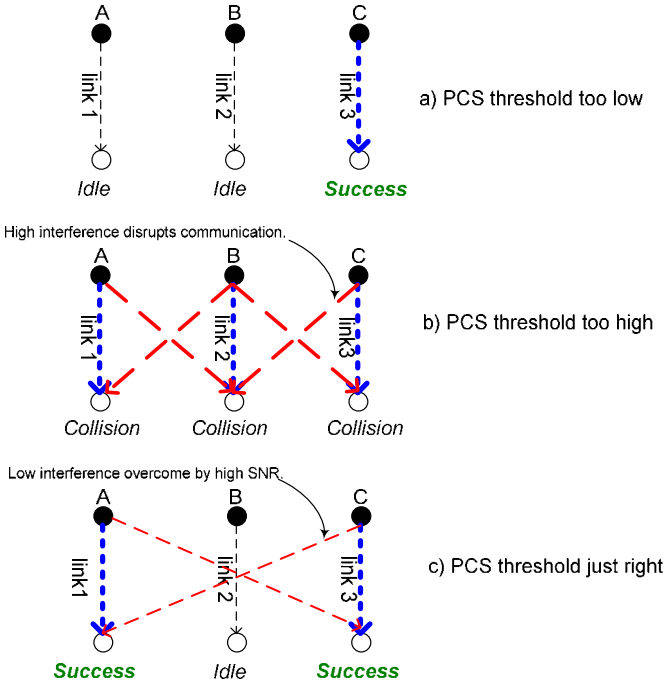

Fig. 3. Physical Carrier Sensing (PCS) and Spatial Reuse.

simultaneously while node B will be forced to back off to prevent packet collisions. When the PCS threshold is optimized, maximal spatial reuse can be achieved without permitting packet collisions.

When properly tuned, PCS is more robust than VCS, because it does not require control packets to be received and correctly decoded. It is also more flexible, since the PCS sensing range can be easily adjusted by tuning the PCS threshold. In Fig.2, all potentially interfering nodes, including node C, can be eliminated by enlarging the PCS sensing range to cover the entire potential interference area, i.e.

$$X \geq D + I. \tag{7}$$

Combining Eq.7 with Eq.5, we obtain

$$X \geq D(1 + S_0^{1/\gamma}), \tag{8}$$

that leads to

$$p_{cs\_t} \leq \frac{1}{(1 + S_0^{1/\gamma})^\gamma}. \tag{9}$$

A potential downside of this approach is the *exposed terminal problem* [10]. For example, in Fig. 2 even though a transmission by node E will not disrupt RX, E will defer its transmission because it lies within the sensing range. Having too many exposed terminals can potentially reduce the overall network throughput. However, by tuning the physical carrier sensing threshold, we will demonstrate a good tradeoff between solving the hidden terminal problem and exacerbating the exposed terminal problem, thereby obtaining high aggregate throughput.

B. Estimating Optimal PCS Threshold to Maximize Spatial Reuse

As already motivated by the earlier example, choosing the optimal PCS threshold can maximize spatial reuse leading to increased aggregate network one-hop throughput. In order to establish some preliminary guidelines for the choice of an optimal PCS threshold, we assume a homogeneous network with identical interference environment at each node [3]. The optimal spatial reuse is achieved when the number of simultaneous successful transmissions reaches the maximum. For successful reception at a receive node, the net interference and noise cannot exceed the tolerable level according to Eq.2,

$$P_I + P_N \leq P_D/S_0, \tag{10}$$

With the assumption that the transmitter and the receiver perceives the same interference and noise level, the optimal PCS threshold should satisfy

$$P_C \leq P_D/S_0, \tag{11}$$

for successful simultaneous transmissions. Hence, P_D/S_0 is the optimal PCS threshold for maximum spatial reuse; a higher P_D/S_0 implies more simultaneous transmissions and greater reuse. The corresponding optimal p_{cs_t} denoted as β, is then

$$\beta = \frac{1}{S_0} \tag{12}$$

independent of path loss exponent γ.

Recall Eq.9 that provides a necessary condition for completely eliminating the interference from hidden nodes. The ratio ρ of the exposed terminal area to the whole PCS sensing area is given by

$$\rho = \frac{\pi X^2 - \pi I^2}{\pi X^2} \approx \frac{D^2(1 + S_0^{1/\gamma})^2 - D^2 S_0^{2/\gamma}}{D^2(1 + S_0^{1/\gamma})^2} = 1 - (\frac{S_0^{1/\gamma}}{1 + S_0^{1/\gamma}})^2. \tag{13}$$

When $S_0^{1/\gamma}$ is small, ρ is not negligible; but for $S_0^{1/\gamma} >> 1$ [4], we have $\rho \approx 0$ so that the exposed terminal problem can be ignored, and Eq.9 reduces to $p_{cs\_t} \leq \beta$.

C. Analysis Model for Aggregate Throughput Limits

In [7], spatial reuse for a homogeneous ad-hoc environment was investigated where every transmitter uses the same transmission power and data rate, and communicates to an immediate neighbor at the constant T-R distance d. The spatial reuse can be characterized by the distance between neighboring simultaneous transmitters (T-T separation). The optimal spatial reuse (min. T-T separation) for two regular network topologies: the 1-D chain network and the 2-D grid network were derived. Let k denote the T-T distance (also

[3]Clearly, this assumption is a main drawback of the subsequent analysis, but further refinements are not possible without assuming specific network topologies. The results here thus have the advantage of not being tied to a specific topology.

[4]More so for higher data rates since higher S_0 values will be required.

called spatial reuse factor) measured in number of hops (hop distance d equals inter-node separation), then k must satisfy

$$\begin{cases} k \geq \left[2\left(1+\frac{1}{\gamma-1}\right)S_0\right]^{\frac{1}{\gamma}}, & \text{Chain network} \\ k \geq \left[6\left(1+\frac{1}{\gamma-2}\right)S_0\right]^{\frac{1}{\gamma}}, & \text{2-D grid} \end{cases} \quad (14)$$

We assume that a suitable MAC protocol schedules simultaneous communication only for transmitters that are k hops away; the network then reaches its aggregate throughput limit. In a chain network of N nodes, a packet must be relayed by each of the $N-2$ intermediate nodes in order to be routed from one end to the other. Since at most N/k simultaneous transmitters can be supported in the chain, the end-to-end throughput C_{e2e} is approximated by

$$C_{e2e} \approx \frac{W}{N} \times \frac{N}{k} = \frac{W}{k} \quad (15)$$

where W denotes the link capacity.

V. A Multi-Channel Two-Radio Architecture with Clustering

A multi-channel architecture with clustering was previously studied in [23], which only considered a centralized TDMA MAC and one radio. Here, we propose to integrate two 802.11 radios (*default* and *secondary*) per node: the default radio is used for inter-cluster communications; while the secondary radio is for intra-cluster communications. Unlike most existing multi-channel approaches, the new clustered multi-channel two-radio (CMT) architecture not only eliminates the need for switching channels on a packet-by-packet basis, but is also fully compatible with legacy devices. Fig.4 shows an example of a mesh network using the CMT architecture with three orthogonal channels, where each circle represents an independent cluster.

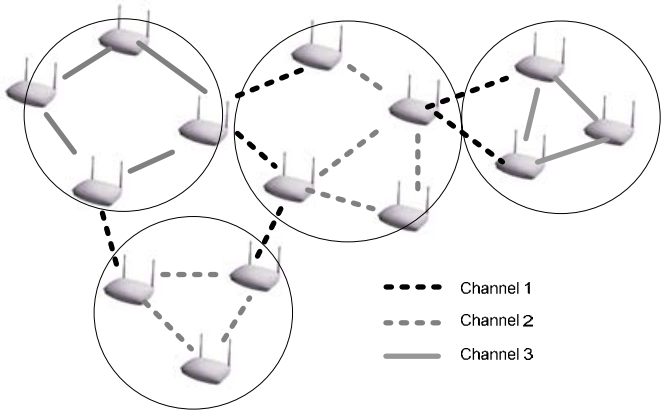

Fig. 4. Clustering Multiple Channels Architecture with Two Radios

Fig. 5 shows protocol stack in a two-radio device. We highlight the two new modules - MAC Extension and Secondary MAC/PHY - needed to enable the two-radio functionality. Algorithms in the new architecture are implemented in the MAC Extension. The secondary MAC/PHY has no administrative functionality, such as association, authentication etc. and can transmit only data traffic.

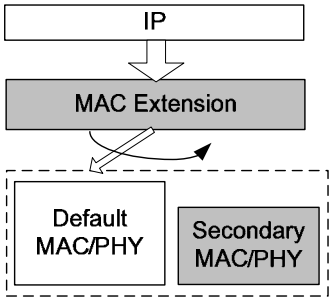

Fig. 5. Two-Radio Protocol Stacks

Clustering is accomplished by using the Highest-Connectivity Cluster (HCC) algorithm first proposed in [22], based on the following rules:

- A node is elected as a clusterhead if it is the most highly connected (having the highest number of neighboring nodes) node of all its "uncovered" neighbor nodes (in case of a tie, lowest ID (e.g. MAC address) prevails);
- A node which has not elected its clusterhead is an "uncovered" node, otherwise it is a "covered" node;
- A node which has already elected another node as its clusterhead gives up its role as a clusterhead.

To minimize the co-channel interference (CCI) among clusters, we propose a Minimum Interference Channel Selection (MIX) algorithm, by which a clusterhead selects the secondary radio channel (denoted as k) with the minimum energy on air for intra-cluster communication.

Let $\bar{E}_i$ denote the average energy on the ith channel for the duration T, we have

$$\bar{E}_i = \frac{\int_{t=t_0}^{t_0+T} E_i(t)dt}{T}, \quad (16)$$

where $E_i(t)$ is the instantaneous energy on the ith channel at time t. Hence, the MIX algorithm is represented by

$$\{k \mid \bar{E}_k = \min(\bar{E}_i | i = \{1, 2, ..., n\})\}, \quad (17)$$

where n is the total number of orthogonal channels. Obviously, the longer the estimation duration T, the more accurate the estimation. Our simulations used T = 2 seconds.

A clusterhead will generate a pseudo random number with 6 bits length for the ID of its cluster. Also it is responsible for notifying all its members which channel is used to configure the secondary radio as well as when the channel information is expired (denoted as T_E (Eq.18)).

$$T_E = T_o + T_1 + \text{uniform}(0,\ T_2), \quad (18)$$

where T_o indicates the time when the clusterhead selected the channel, and T_1 and uniform$(0,\ T_2)$ [5] give the constant and random components of the lifetime, respectively. Our simulations used $T_1 = T_2 = 100$ seconds.

When the channel information is expired, the clusterhead will re-run the MIX algorithm to select a new channel, then

[5]a random variable with uniform distribution on the range $(0, T_2)$; the random component is designed to avoid the event that two clusters always select the channel at the same time, i.e., channel selection collisions.

broadcast the updated channel and its lifetime to its cluster members.

After getting the channel information, the neighboring nodes notify each other the channel used by their secondary radio. Thereby, we build a new 16-bit CMT field (see Fig.6) with three sub-fields: status, channel, and number of uncovered neighboring nodes. The "cluster-ID" flag indicates the cluster that the node belongs to, and is only meaningful when "status" is not "uncovered"; the "number of uncovered neighboring nodes" is used for electing clusterhead. In our OPNET implementation, the new 16-bit CMT field is added into the 802.11 DATA frame. The 16-bit "Duration ID" field in the legacy 802.11 ACK frame can also be used as the new CMT field, since it is meaningless when segmentation is not used or the ACK is for the last fragment of the packet.

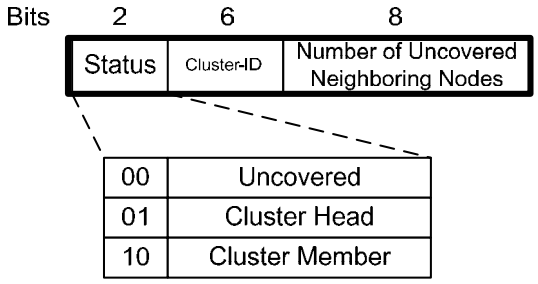

Fig. 6. Definition of 16-Bit CMT Field

After learning that a peer node belongs to the same cluster, a node will configure the forwarding table in its extended MAC such that all packets destined to the peer node go through the secondary MAC/PHY module. Fig.7 summarizes the above clustering and channel selecting procedures with a state transition diagram.

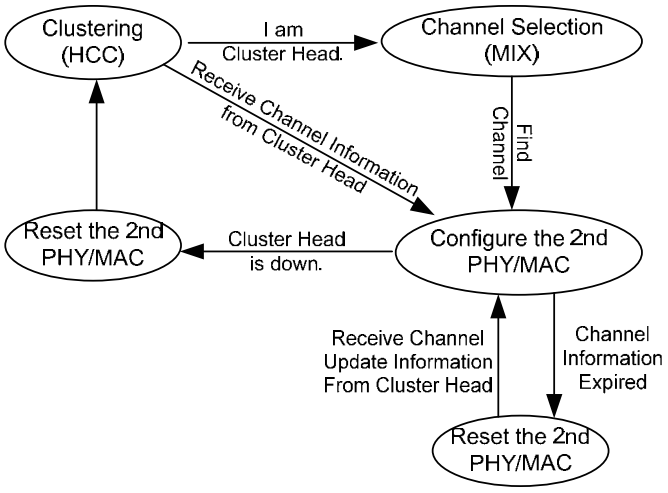

Fig. 7. A State Transition Diagram of Clustering and Channel Selecting Procedures

VI. Simulation Results and Discussions

In this section, we present results from a series of simulations to demonstrate the effectiveness of physical carrier sensing with tunable sensing thresholds in improving network performance for various topologies. All the simulations were conducted in the OPNET simulation environment [15]. We have extended OPNET kernel modules to support tunable physical carrier sensing, a configurable propagation environment and multiple 802.11b data rates.

In all simulations, we configured each node to be always backlogged with 1024 bytes long MAC data frames. Each node transmits at a fixed power of 0 dbm. By default, the OPNET simulator configures the physical carrier sensing threshold to be the same as the reception threshold P_R. Furthermore, the ambient noise level was set at -200 dBm.

The primary performance metric studied in this paper is throughput, defined as the total number of bits successfully received in a second. As per the .11 MAC, if the sender does not receive an ACK for a transmitted data packet, it assumes that the data packet is lost and performs a retransmission. However, it is also possible that the data packet is received correctly, but the ACK is lost. This also causes a retransmission and can result in a multiple copies of the same data packet at the receiver. In this case, only the first one received will be forwarded up to higher layers, and the rest discarded. When computing throughput in this paper, we only count successful non-duplicate data packets , i.e. the *goodput* which underestimates the actual throughput on the physical channel of the network. However, since ACK packets are much shorter than data packets and they are typically transmitted using the lowest (most reliable) data rate in 802.11, the probability of successfully receiving a data packet but losing an ACK packet is very low. Thus, we assume that *throughput* is approximately equal to *goodput* in an 802.11 network.

Note that the .11 MAC employs contention management via the binary exponential backoff (BEB) with a configurable contention window (CW) size parameter. This random scheduling of user transmissions naturally impacts the received SINR in addition to the various mechanisms described in this paper. Since the primary focus of the simulations in this section is on interference avoidance via PCS, the BEB mechanism is disabled in our simulations and the contention window size is fixed at the maximum value for 802.11b (CW = 1024) to minimize the likelihood of collisions due to simultaneous transmission. This configuration allows us to isolate the specific effects of adaptive physical carrier sensing on network performance.

A. Point-to-point baseline performance of 802.11b MAC

To validate the effectiveness of physical carrier sensing, we need the following two baseline figures: the SINR thresholds (S_0) required to sustain each available data rate in an 802.11b network, and the effective MAC throughput at each data rate. In the first simulation, we configured a network of two nodes – one sender and one receiver. The pathloss exponent was set to 2 to reflect a free-space environment. With RTS/CTS disabled, we varied the T-R separation distance and measured the effective throughput provided by the MAC layer at the receiver. The same simulation sequence was repeated for all four data rates defined in the 802.11b standard.

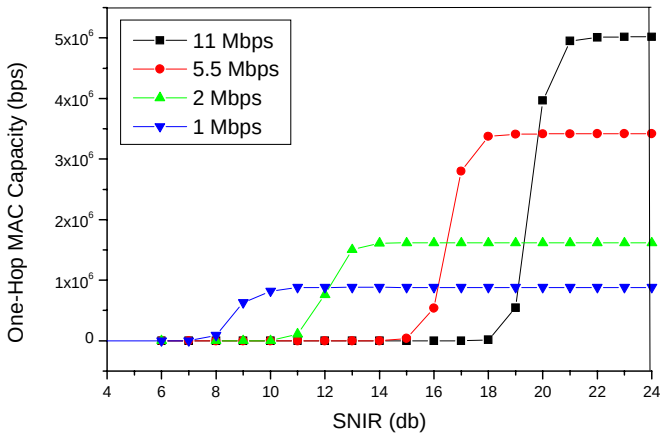

Fig. 8. One-Hop multi-rate performance of 802.11b for various SINR values at the receiver (RTS/CTS disabled).

Data Rate (Mbps)	1	2	5.5	11
S_0 (dB)	11	14	18	21
W (Mbps)	0.89	1.5	3.5	5.0

TABLE II

ONE-HOP PERFORMANCE OF 802.11B MAC WITHOUT RTS/CTS

The results are shown in Fig.8 where instead of the T-R distance, the throughput is shown against the SINR at receiver. Hence the results depict the fundamental relationship between MAC throughput and receiver SINR. This mapping is valid irrespective of pathloss, transmission power and T-R distance. These results, recorded in Table II, will be used to design and analyze simulations in the rest of the section. The results confirm that MAC overhead is generally larger at higher data rates and higher data rates require higher SINR thresholds, as expected.

B. Maximizing Spatial Reuse with the Optimal PCS

We conduct simulations in two scenarios with regular topology: 90-node chain and 10×10 grid. The goal is to validate the theoretical optimal PCS threshold β, derived in Section IV-B.

First, we expanded the previous network into a chain of 90 nodes (to approximate an infinite chain). The only traffic allowed is originated by node 1 and designated for node 90, with the other 88 intermediate nodes acting as relays. The reception power threshold (P_R) was configured such that the transmission range is 13 meters. Each node relied on physical carrier sensing only to avoid interference using identical carrier sensing threshold and data rates. We measured the end-to-end throughput while varying the sensing threshold and the data rate. The results for $\gamma = 2$ are plotted in Fig. 9.

Note that the results show the existence of an optimal sensing threshold value for each data rate. With everything else fixed, altering the data rate changes the SINR requirement (S_0), hence the optimal sensing threshold changes as well. Also notice that the common practice of having the carrier sense threshold equal to the reception threshold, i.e., $P_{cs\_t} = 0db$ corresponds to the right-most point on respective curves. Hence, the throughput improvement achieved by tunable physical carrier sensing threshold can be as high as 4 times (at data rate 11 Mbps).

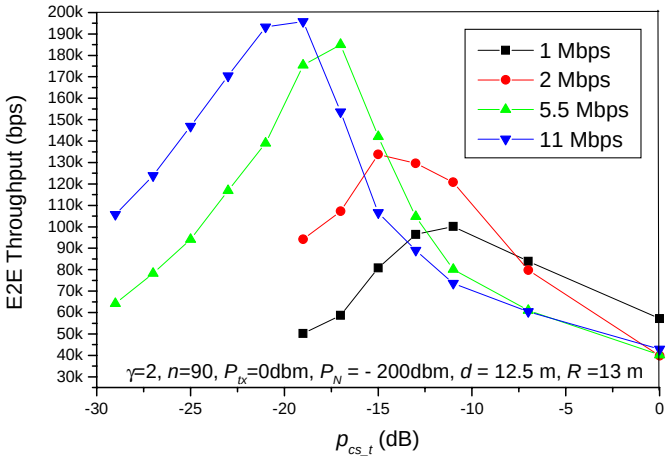

Fig. 9. End-to-end throughput in a 90-hop chain for various sensing thresholds and data rates.

Table III compares the optimal sensing threshold p_{cs_t} obtained from the simulations against the theoretical optimum β. As the table shows, the two values matches very well.

Data Rate (Mbps)	1	2	5.5	11
β (theoretical Eq.12)	-11	-14	-18	-21
Simulation	-11	-15	-17	-19

TABLE III

OPTIMAL CARRIER SENSING THRESHOLDS (DB) IN A 90-NODE CHAIN

Table IV compares the optimal throughputs obtained from the simulations against the prediction from the spatial reuse study described in Sec.III-C. The theoretical prediction assumed a perfect MAC protocol that always derives the globally optimal schedule for communications; this yields a theoretical upper-bound of network throughput. As shown in Table IV, the network with optimally tuned physical carrier sensing was able to achieve around 90% of the theoretical maximum.

Data Rate (Mbps)	1	2	5.5	11
W (Mbps)	0.89	1.5	3.4	5.0
k (spatial reuse)	7.1	10	15.9	22.4
T: Theoretical (Eq.15)	0.105	0.15	0.21	0.223
S: Simulation	0.1	0.134	0.185	0.196
S/T	95%	89%	88%	88%

TABLE IV

OPTIMAL E2E THROUGHPUT IN A 90-NODE CHAIN

Next, we turn to a 2-D network: 10×10 grid, which is more representative of typical real world topologies. Each packet has its own destination chosen randomly from the immediate neighbors of the transmitter. In this configuration, the Manhattan distance between neighboring nodes

was 4.5 meters. The reception power threshold (P_R) was configured to allow the transmission range of only 4.5 meters such that only immediate neighbors could directly communicate.

We conducted four sets of simulations using 1 Mbps, 2 Mbps, 5.5 Mbps and 11 Mbps as the data rate for each node, respectively. In each set of the simulations, we altered the path loss exponent and PCS threshold. The aggregate throughput of the grid network are plotted in Fig. 10. It is evident that the optimal PCS threshold does not change with the path loss exponent in a large homogeneous network, and the optimal PCS threshold obtained via simulation matches the theoretical β very well (see Table V).

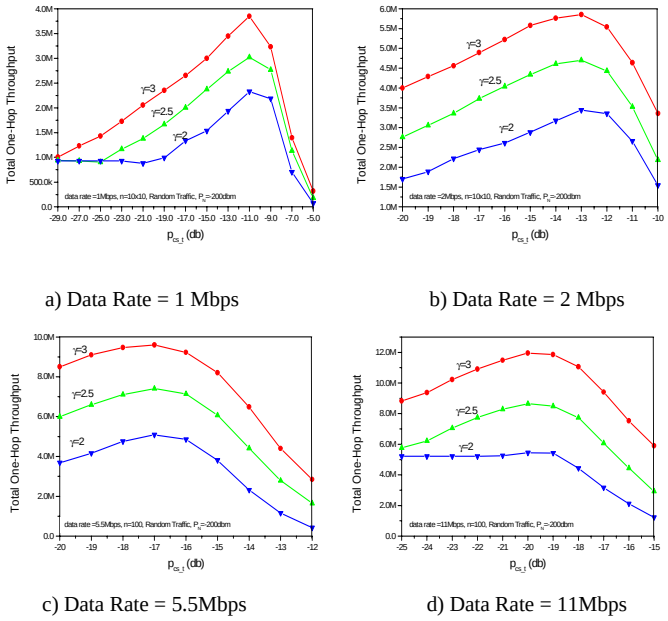

Fig. 10. Aggregate 1-hop throughput as a function of PCS threshold for various pathloss exponent values in a 10×10 802.11b grid

Data Rate (Mbps)	$\gamma = 2$	$\gamma = 2.5$	$\gamma = 3$	β
1	-11	-11	-11	-11
2	-13	-13	-13	-14
5.5	-17	-17	-17	-18
11	-19	-20	-20	-21

TABLE V

SIMULATION RESULTS OF OPTIMAL CARRIER SENSING THRESHOLDS (DB) IN A 10×10 802.11B GRID

The simulation is now repeated for 802.11a [6]. Table VI compares the theoretical optimal p_{cs_t} (i.e. β) with the optimal value from simulations, showing that the theoretical optimal carrier sensing threshold β is also valid for 802.11a network.

C. Optimal PCS + Multi-Channel Clustering

Fig. 11 shows an example of how our clustering multi-channel and two-radio architecture works in a 10×10 regular grid with three orthogonal channels. We implement a two-radio 802.11 client module in OPNET. Let d denote the distance between two nearest neighbors; we configure the transmission range as $\sqrt{2}d$. During the simulation, the network will automatically cluster into the topology as shown in Fig.11. The dark nodes are clusterhead, and the dotted circle indicates all independent clusters. Two orthogonal channels (for the circles denoted by thick and thin dash lines, respectively) are used for intra-cluster communications. The channel assignment in Fig.11 minimizes co-channel interference and achieves the highest spatial reuse.

[6]We use the same modulation curve for 802.11a simulation as in [18]

Data Rate	6	9	12	18	24	36	48	54
β	-7	-9	-11	-13	-17	-22	-27	-29
Simulation	-7	-9	-11	-13	-17	-21	-27	-29

TABLE VI

OPTIMAL CARRIER SENSING THRESHOLDS (DB) IN A 10×10 802.11A GRID WITH DIFFERENT DATA RATE (MBPS) ($\gamma = 3$)

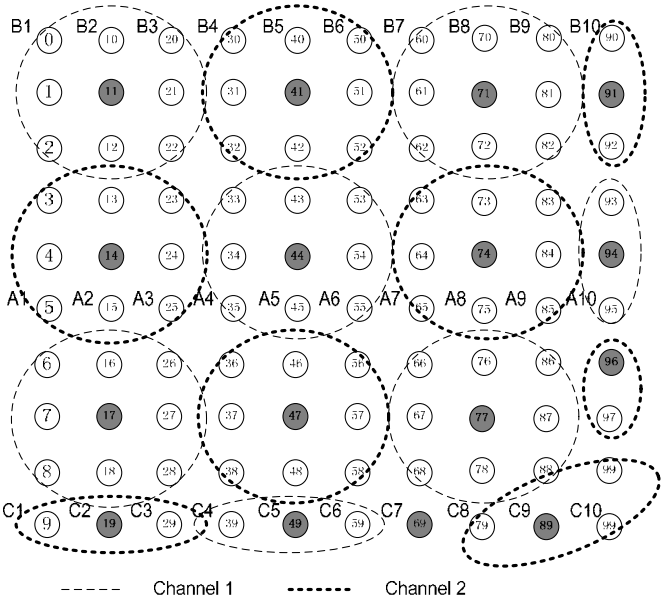

Fig. 11. An Example of 10×10 Grid Using the Clustering Multi-Channel and Two-Radio Architecture

Fig.12 compares the total one-hop throughput with the new clustering multi-channel and two-radio architecture to the traditional single-channel, single-radio mesh. A random traffic generation model at each node was used with a sufficiently high offered load such that the nodes remain saturated during the simulation. Fig.12 clearly demonstrates the performance improvement with clustering and multiple orthogonal channels. The steady-state average throughput is 8.1 Mbps in the new CMT architecture, and only 2.7 Mbps in the single-channel and single-radio mesh. The gain is about 300%, which is the maximum gain achievable when using 3 orthogonal channels.

Fig.13 illustrates the one-hop throughput distribution with respect to links, where links A_i, B_i, and C_i are also indicated in Fig. 11 ($i = \{1, 2, ..., 10\}$). Clearly, links A_i experience worse interference environment than links B_i and

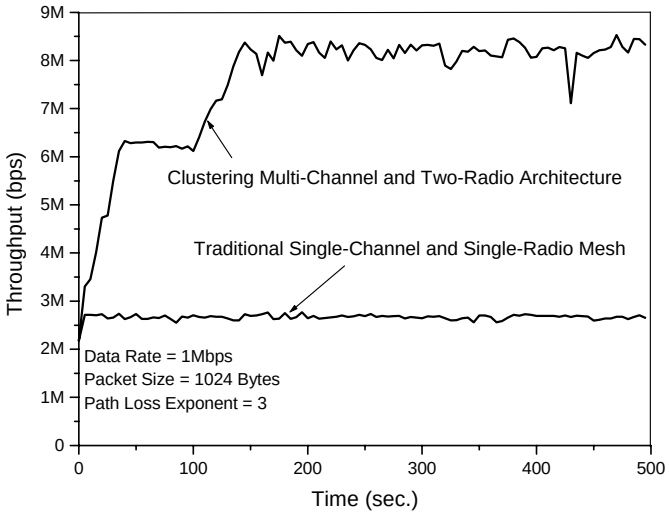

Fig. 12. Total One-Hop Throughput Comparison

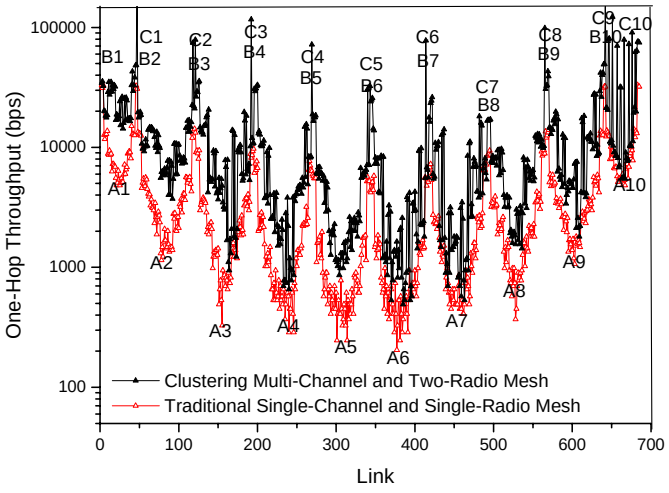

Fig. 13. Average One-Hop Throughput Distribution (between 300sec. and 500 sec.)

C_i, leading to the oscillation of the throughput distribution, illustrating the *location-dependent fairness* problem. We do not consider the fairness problem further; it is interesting to speculate how physical carrier sensing may be used to mitigate the *location-dependent fairness* problem. It implies for instance that the preferable locations for gateways in a wireless mesh network may not be the center of the network.

Finally, we validate the new architecture in a random topology as shown in Fig.14. The transmission range is fixed at 25 meters. We color-coded the graph in Fig.14. Red and blue indicates the nodes using channel 1 and channel 2 for their secondary radio, respectively; while black nodes are the single-node clusters. We also used the circles to illustrate the clusters with clusterhead in the center. Fig.15 compares the performance with both aggregate throughput and throughput distribution. We clearly see that (after 300 seconds) the aggregate throughput of the proposed architecture (10Mbps) is almost 3 times higher than that of the traditional one (3.5Mbps).

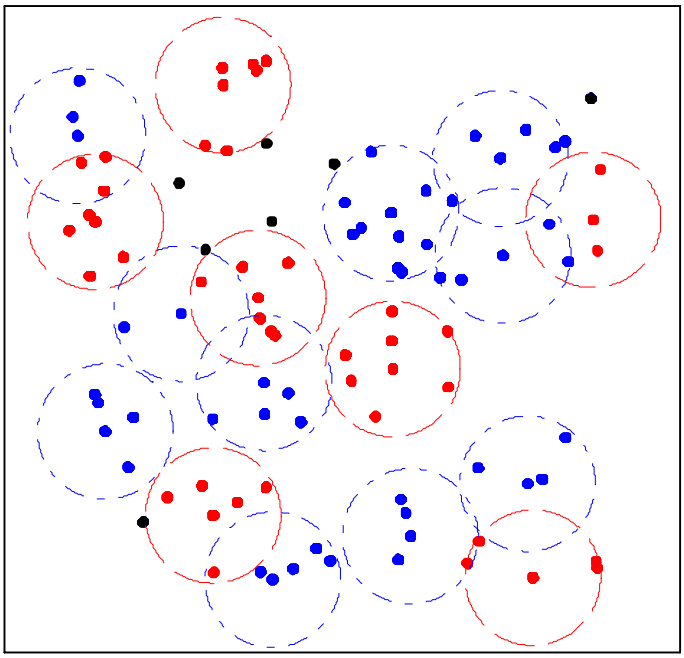

Fig. 14. 2D 200m x 200m 100-Nodes Random Topology Using the Clustering Multi-Channel and Two-Radio Architecture (at 500 seconds)

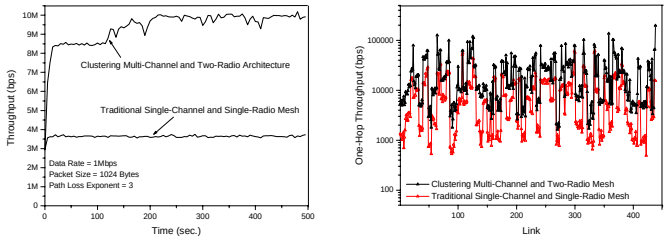

a) Tracing Aggregate Throughput b) Throughput Distribution

Fig. 15. Performance Comparison in the Random Topology

VII. Conclusion

In this paper, we propose to enhance physical carrier sensing with a dynamically tunable sensing threshold and adopt a novel clustering two-radio and multi-channel architecture to improve spatial reuse in 802.11 mesh networks, aiming at increasing the aggregate network throughput. Simulations were performed for both 1-D chain and 2-D grid topologies to validate the analysis and the proposed scheme. The main contributions of this paper are:

(1) We have demonstrated that physical carrier sensing with the tunable sensing threshold is effective at leveraging spatial reuse in 802.11 multi-hop mesh networks, shown by increases in aggregate throughput. This improvement is achieved without requiring the use of virtual carrier sensing. Although the 802.11 MAC is a CSMA/CA based distributed and asynchronous scheme, it has the capability to make good use of the spatial-reuse property in a mesh (90% of the theoretical limit in a chain).

(2) We have proposed an adaptive PCS scheme to achieve a near-optimal carrier sense threshold au-

tomatically, leading to a substantial throughput improvement for 802.11 mesh networks. With assumptions of homogeneous links and co-location of sender and receiver, $1/S_0$ gives the theoretical approximation to the optimal sensing threshold, where S_0 is the SINR threshold for achieving the link capacity.

(3) We have presented a new clustering multi-channel and two-radio (CMT) architecture using 802.11 MAC protocols. Distributed clustering works with a new minimum interference channel selection algorithm (MIX) to distribute orthogonal channels in a mesh, maximizing the aggregate throughput. OPNET simulations were conducted to validate the new architecture. Compared to a traditional single-channel and single-radio mesh, the gain achieved with three orthogonal channels in terms of the aggregate one-hop throughput is about 300% in a 10×10 grid using local, random, and saturate traffic as well as in a 200m x 200m 100-nodes random topology.

Although this paper is focused on 802.11 networks, the analysis on optimal physical carrier sensing is applicable to any CSMA/CA-based mesh network. As the initial step to showcase the potential of enhanced physical carrier sensing and multi-channel clustering in improving aggregate throughput, this paper focuses on regular network topologies. Future work may include extending the investigation to random topologies.

ACKNOWLEDGEMENT

The work of Jing Zhu and Sumit Roy was supported in part by an Intel Research Council Grant.

REFERENCES

[1] IEEE Standard for Wireless LAN Medium Access Control (MAC) and Physical Layer (PHY) specifications, ISO/IEC 8802-11: 1999(E), Aug. 1999.
[2] MeshDynamics, http://www.meshdynamics.com.
[3] MeshNetworks, http://www.meshnetworks.com.
[4] Packethop, http://www.packethop.com
[5] B. P. Crow, J. G. Kim, IEEE 802.11 Wireless Local Area Networks, IEEE Comm. Mag., Sept. 1999.
[6] G. Bianchi, Performance Analysis of the IEEE 802.11 Distributed Coordination Function, IEEE JSAC, vol. 18, no. 3, March 2000.
[7] X. Guo, S. Roy, W. Steven Conner, Spatial Reuse in Wireless Ad-Hoc Networks, VTC2003.
[8] X. Guo, "Personal research notes", 2003.
[9] A. Adya, P. Bahl, J. Padhye, A. Wolman and L. Zhou, 'A Multi-radio Unification Protocol for IEEE 802.11 Wireless Networks," Tech. Rpt. MSR-TR-2003-44, July 2003.
[10] D. Shukla, L. Chandran-Wadia, S. Iyer, Mitigating the exposed node problem in IEEE 802.11 adhoc networks, IEEE ICCCN 2003, Dallas, Oct 2003.
[11] F. A. Tobagi, L. Kleinrock, Packet Switching in Radio Channels: PART II- The Hidden Terminal Problem in Carrier Sensing Multiple Access and Busy Tone Solution", IEEE Trans. on Commun, Vol. COM-23, No. 12, pp. 1417-1433, 1975.
[12] K. Xu, M. Gerla, S. Bae, How effective is the IEEE 802.11 RTS/CTS handshake in ad hoc networks?, GLOBECOM02, Nov 17-21, 2002.
[13] S. Xu, T. Saadawi, Does the IEEE 802.11 MAC Protocol Work Well in Multihop Wireless Ad Hoc Networks? IEEE Communications Magazine, P130-137, June 2001.
[14] F. Ye, B. Sikdar, Improving Spatial Reuse of IEEE 802.11 Based Ad Hoc Networks, To appear in the Proceedings of IEEE GLOBECOM, San Francisco, December 2003.
[15] http://www.opnet.com
[16] Intersil, Direct Sequence Spread Spectrum Baseband Processor, Doc# FN 4816.2, Feb. 2002, http://www.intersil.com/
[17] V.Bharghavan, A. Demers, S. Shenker, and L. Zhang, MACAW: A Media Access Protocol for Wireless LANs, in Proc. Of ACM SIGCOMM'94,
[18] A.J. van der Vegt, Auto rate fallback algorithm for the ieee 802.11a standard, http://www.phys.uu.nl/ vdvegt/docs/gron/.
[19] Theodore S. Rappaport. Wireless Communications, Principles and Practices, 2nd Ed. Prentice Hall, 2002. ISBN 0-13-042232-0
[20] J. Monks, V. Bharghavan, W. Hwu, A Power Controlled Multiple Access Protocol for Wireless Packet Networks, in IEEE INFOCOM, April 2001.
[21] R. Roy Cloudhury, X. Yang, R. Ramanathan and N. H. Vaidya, Using Directional Antenna for Medium Access Control in Ad Hoc Networks, in ACM MOBICOM, Atlanta, GA, Sept. 2002.
[22] M. Gerla and J.T.-C. Tsai, "Multicluster, mobile, multimedia radio network", ACM/Baltzer Journal of Wireless Networks. vol. 1, (no. 3), 1995, p. 255-265.
[23] C. R. Lin, M. Gerla, "Adaptive Clustering for Mobile Wireless Networks," IEEE Jour. Selected Areas in Communications, pp. 1265-1275, Sept. 1997.
[24] Y. P. Chen and A. L. Liestman, "A Zonal Algorithm for Clustering Ad Hoc Networks", International Journal of Foundations of Computer Science, 2003.
[25] N. Jain and S. Das, A Mutlichannel CSMA MAC Protocol with Receiver-Based Channel Selection for Mutlihop Wireless Networks, in Proceedings of the 9th Int. Conf. on Computer Communications and Networks (IC3N), Oct. 2001.
[26] S.-L. Wu, C.-Y. Lin, Y.-C. Tseng and J.-P. Sheu, A New Mutli-Channel MAC Protocol with On-Demand Channel Assignment for Multi-Hop Mobile Ad Hoc Networks, in IEEE Wireless Communications and Networking Conference (WCNC), Chicago, IL, Sept. 2000.
[27] A. Adya, P. Bahl, J. Padhye, A. Wolman, and L. Zhu, A Multi-Radio Unification Protocol for IEEE 802.11 Wireless Networks, Microsoft Research, Technical Report MSR-TR-2003-44, July, 2003.